

Pyridine Inhibitor Binding to the 4Fe-4S Protein *A. aeolicus* IspH (LytB): A HYSCORE Investigation

Weixue Wang,[†] Jikun Li,[†] Ke Wang,[‡] Tatyana I. Smirnova,[§] and Eric Oldfield^{*,†,‡}

[†]Center for Biophysics and Computational Biology, 607 South Mathews Avenue, and [‡]Department of Chemistry, 600 South Mathews Avenue, University of Illinois at Urbana–Champaign, Urbana, Illinois 61801, United States

[§]Department of Chemistry, North Carolina State University, 2620 Yarbrough Drive, Raleigh, North Carolina 27695, United States

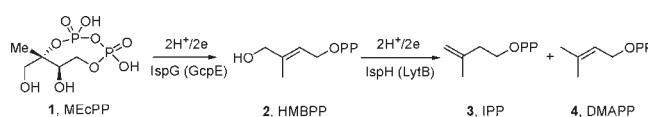
S Supporting Information

ABSTRACT: IspH is a 4Fe-4S protein that carries out an essential reduction step in isoprenoid biosynthesis. Using hyperfine sublevel correlation (HYSCORE) spectroscopy, we show that pyridine inhibitors of IspH directly bind to the unique fourth Fe in the 4Fe-4S cluster, opening up new routes to inhibitor design, of interest in the context of both anti-bacterial as well as anti-malarial drug discovery.

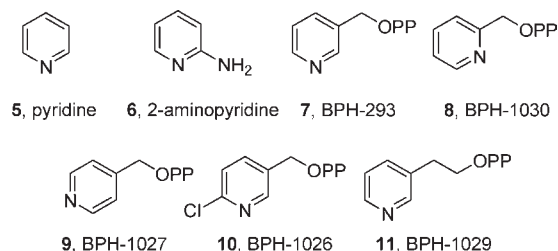
Isoprenoid biosynthesis is an important target for drug discovery.¹ In most pathogenic bacteria as well as in malaria parasites, the early stages in isoprenoid biosynthesis are carried out by the methylerythritol phosphate pathway.² This pathway is essential for producing the isoprenoids used in, e.g., cell wall biosynthesis in bacteria and in quinone formation, and, since it is not present in humans, the enzymes involved are important targets for the development of new antibiotics.³ The last two enzymes, IspG and IspH, are unusual 4Fe-4S-containing proteins that carry out $2\text{H}^+ / 2\text{e}^-$ reductions of the substrates 2-C-methyl-D-erythritol-2,4-cyclo-diphosphate (MEcPP, **1**)^{4–6} and *E*-1-hydroxy-2-methylbut-2-enyl-4-diphosphate (HMBPP, **2**) to form the C₅ isoprenoids isopentenyl diphosphate (IPP, **3**) and dimethylallyl diphosphate (DMAPP, **4**) in an ~1:5 ratio,^{7,8} as shown in Scheme 1.

In recent work we proposed that both the IspG (EC 1.17.7.1, HMBPP synthase, also known as GcpE)⁹ and the IspH (EC 1.17.1.2, HMBPP reductase, also known as LytB)-catalyzed reactions involve formation of organometallic species (i.e., containing Fe–C bonds).¹⁰ Support for the intermediacy of organometallic species in catalysis comes indirectly from electron paramagnetic resonance (EPR) and electron nuclear double-resonance (ENDOR) spectroscopy as well as mechanistic considerations¹⁰ and, more directly, from the observation that the Fe–C distances (2.6–2.7 Å) between the apical iron atom in the 4Fe-4S cluster and the allylic species seen crystallographically in IspH are even shorter than the ones observed for bound HMBPP¹¹ and far shorter than the 3.6–3.7 Å sum of the Fe, C van der Waals radii.¹² We also found that alkynes could be quite potent inhibitors of both IspG and IspH, and EPR and ENDOR spectra indicated that these alkynes bound at or very close to the unique fourth Fe in the reduced 4Fe-4S cluster. The ability to inhibit IspG or IspH is of interest in the context of the development of anti-infectives, and the ability of a given compound to inhibit both enzymes is of even more interest because, in principle, it will lead to a decrease in drug resistance since both enzymes would be required to mutate.

Scheme 1. Reactions Catalyzed by the Proteins IspG (GcpE) and IspH (LytB)



Scheme 2. Aromatic Species Investigated



In addition to alkyne inhibitors, we discovered a second class of IspH inhibitors, pyridine diphosphates,¹³ but how these bound to the protein was not clear. Here, we report the results of X-band hyperfine sublevel correlation (HYSCORE) spectroscopic and quantum chemical investigations, which help clarify how these inhibitors function.

We first investigated a series of pyridine ligands, **5**–**11** (Scheme 2), binding to wild-type IspH from *Aquifex aeolicus*. The continuous-wave EPR spectrum of IspH + pyridine (**5**) is the same as that of the unliganded protein (i.e., in the absence of pyridine, Supporting Information Figure S1a), and there is no evidence for any sizable pyridine-¹⁴N hyperfine interaction in the HYSCORE spectrum (Figure S1b), indicating only very weak binding affinity to IspH. The same results are obtained with the more basic (pK_a = 6.8 vs 5.2) species 2-aminopyridine (**6**, Figure S1c). However, on addition of the inhibitor BPH-293 (**7**, IC₅₀ = 38 μM), the EPR spectrum changes¹³ (Figure S1a) and new signals attributable to ¹⁴N single- and double-quantum transitions appear in the (+,–) quadrant of the HYSCORE spectrum (Figure 1a). The ¹⁴N hyperfine interaction is quite large, with the hyperfine coupling constant being ~8 MHz. Reconstituted IspH (Figure 1a) and anaerobically purified IspH (Figure S2)

Received: January 27, 2011

Published: April 12, 2011

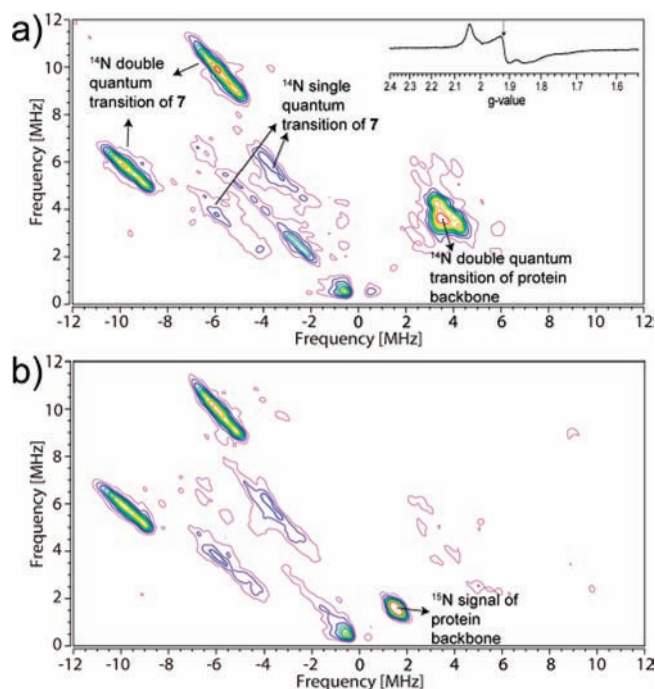
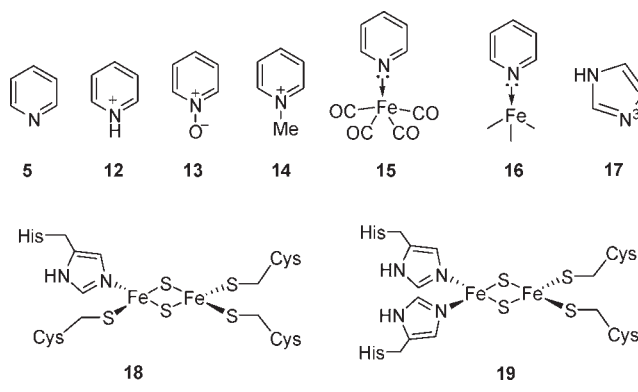


Figure 1. HYSCORE spectra of *A. aeolicus* IspH + pyridine inhibitor 7. (a) HYSCORE spectra of unlabeled *A. aeolicus* IspH + 7. The inset shows the CW-EPR spectrum, and the arrow indicates the magnetic field position for collecting the HYSCORE data. (b) HYSCORE spectra of ^{15}N -labeled *A. aeolicus* IspH + 7. Microwave frequency: (a) 9.66 and (b) 9.68 GHz. Magnetic field was set at $g_2 = 1.921$, $\tau = 136$ ns.

both give the same results. The *ortho*- and *para*-pyridyl analogues of 7 (compounds 8, $\text{IC}_{50} = 1.2$ mM, and 9, $\text{IC}_{50} = 149$ μM) show no evidence of any sizable pyridine- ^{14}N hyperfine interaction in their HYSCORE spectra (Figure S1d,e), due presumably to their inability to bind to the fourth Fe, for “steric” reasons. Moreover, chlorine substitution of 7 (compound 10) results in loss of all activity ($\text{IC}_{50} > 3$ mM), due presumably to loss in donor ability of the pyridine nitrogen (the computed pK_a values of the pyridine fragments in 7 and 10 are 4.7 and 0.7, respectively), consistent with the absence of a pyridine- ^{14}N HYSCORE signal (Figure S1f). Addition of one CH_2 group to the side chain of 7 results in a better inhibitor (11, $\text{IC}_{50} = 9.1$ μM), although there is no significant difference between the HYSCORE spectra of 7 (Figure 1a) and 11 (Figure S1g), indicating that differences in enzyme inhibition are due to differences in the alkyl diphosphate fragment binding in the active site, rather than differences in Fe–pyridine interactions.

These results do not, however, prove that the ^{14}N HYSCORE signals in the (+,–) quadrant (Figures 1a and S1g) arise directly from the inhibitors 7 and 11 since, in principle, inhibitor binding might result in a protein conformational change and binding of a protein ligand to Fe, e.g., the nearby His 42 or 124, which form part of the active site.¹⁴ To investigate this possibility, we prepared a sample using uniformly ^{15}N -labeled IspH and inhibitor 7. As can be seen in Figure 1b, the ^{14}N signals centered at ~ 3.6 MHz seen in Figure 1a are no longer present and are replaced by a signal centered at 1.5 MHz, the ^{15}N Larmor frequency. Moreover, the ^{14}N signals in the (+,–) quadrant are essentially identical to those seen in samples prepared using unlabeled IspH (Figure 1a). This strongly suggests that the

Scheme 3. Structures Discussed in the Text



signals centered at ~ 3.6 MHz arise from protein nitrogens near the 4Fe-4S cluster, while the ^{14}N signals in the (+,–) quadrant arise from the bound inhibitor 7, rather than from any protein residues.

To begin to better understand the interaction between the pyridine inhibitor 7 and IspH, we next simulated the HYSCORE spectra of IspH + 7 taken at three different magnetic field strengths (Figure S3a–c) using the EasySpin program¹⁵ (Figure S3d–f), finding $a_{\text{iso}}(^{14}\text{N}) = 7.4$ MHz, $A_{\text{ii}}(^{14}\text{N}) = [6.2 \ 7.6 \ 8.4]$ MHz for the hyperfine interaction, and $e^2qQ/h = 3.0$ MHz for the nuclear quadrupole coupling constant.

This large $a_{\text{iso}}(^{14}\text{N})$ is similar to, or even larger than, those of a number of systems in which nitrogens directly bind to Fe centers. For example, in met-myoglobin the porphyrin nitrogens have $a_{\text{iso}} = 8.11$ and 7.8 MHz, and the histidine N_ϵ has $a_{\text{iso}} = 9.28$ MHz.¹⁶ In a model heme complex, $\text{FeTPP}(4\text{-MeIm})_2$ (TPP = tetraphenylporphyrin; 4-MeIm = 4-methylimidazole), the a_{iso} of the porphyrin nitrogens is 5.1 MHz, while that of the coordinated 4-MeIm is 5.7 MHz.¹⁷ In Rieske-type 2Fe-2S proteins, $a_{\text{iso}}(^{14}\text{N})$ of the coordinated His nitrogens is ~ 5 MHz,¹⁸ and in the case of the 4Fe-4S enzyme MoaA (which also has a unique fourth iron), N1 of the substrate guanosine 5'-triphosphate binds to the fourth iron and has $a_{\text{iso}}(^{14}\text{N}) = 3.6$ MHz.¹⁹ On average, these results give an $a_{\text{iso}}(^{14}\text{N}) \approx 6$ MHz for systems containing Fe–N bonds, suggesting that the IspH + 7 complex also contains an Fe–N bond.

The large ^{14}N hyperfine interaction seen in the IspH + 7 complex might also, at least in principle, indicate that the pyridine fragment is just close to the reduced 4Fe-4S cluster, without directly bonding to the fourth iron. For example, the pyridine group might be protonated and interact with, e.g., the E126 CO_2^- group that is close to the cluster, or it could be close by but deprotonated. Fortunately, determination of the ^{14}N nuclear quadrupole coupling constant (e^2qQ/h) enables an answer to this question, since protonated, neutral, and metal-coordinated pyridine ligands have very different e^2qQ/h values.²⁰

For pyridine itself, $e^2qQ/h = 4.6$ MHz, but in species in which there is a formal 1+ charge on N, such as the pyridinium ion (12), pyridine-*N*-oxide (13), and *N*-methylpyridinium (14; see Scheme 3 for structures), e^2qQ/h values of approximately 1 MHz are observed experimentally.²⁰ In the case of pyridine bonded to Fe in $\text{Fe}(\text{CO})_4(\text{pyr})$ (15), e^2qQ/h is in between these extreme values ($e^2qQ/h \approx 2.4$ MHz), and for $\text{Mo}(\text{pyr})_2(\text{CO})_4$ as well as $\text{Cr}(\text{CO})_4(2,2'\text{-bipyridyl})$, $e^2qQ/h \approx 3.1$ MHz. So, when pyr is bonded to Cr, Mo, or Fe, the e^2qQ/h decreases from the 4.6 MHz seen in free pyridine to ~ 2.4 –3.1 MHz, due to metal–ligand

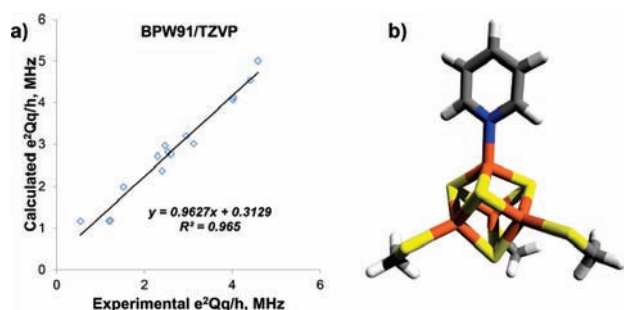


Figure 2. (a) Graph showing correlation between experimental and computed e^2qQ/h values for a series of model systems. (b) Model used in quantum mechanical calculation of the ^{14}N e^2qQ/h value for IspH + 7 complex.

bonding, close to the 3.0 MHz value we find from the ^{14}N HYSCORE results.

To see to what extent these e^2qQ/h values might be reproduced computationally, we used the Gaussian-09 (Revision A.01) program.²¹ Results are given in Table S1 and are shown graphically in Figure 2 and Figure S4. Clearly, there is a good correlation (Figure 2a) between theory and experiment ($R^2 = 0.965$; slope = 0.963) for a series of model systems, and when using $[\text{Fe}_4\text{S}_4(\text{SMe})_3(\text{pyr})]^{2-}$ (**16**, Figure 2b) as a model, we find $e^2qQ/h = 2.3$ MHz for the pyridine ^{14}N , in quite good accord with experiment.

This large decrease in e^2qQ/h , from the 4.6 MHz value found for free pyridine to the 2.4–3.1 MHz values observed in model systems and the IspH + 7 complex, is also seen in proteins in which imidazole (histidine) ligands bind to Fe. For example, for imidazole (**17**), the N3 (deprotonated) e^2qQ/h is 4.032 MHz,²² in good accord with the 3.894 MHz computed using DFT. The e^2qQ/h values for solid imidazole and solid histidine are both smaller and essentially identical (3.27 MHz for Im; 3.36 MHz for His),²³ due presumably to very strong hydrogen bonding in the solid state. But when imidazole and histidine are bound to Fe in metalloproteins, e^2qQ/h decreases considerably from the 4 MHz gas-phase value (for imidazole).

For example, in myoglobins, e^2qQ/h ranges from 2.2 to 2.5 MHz for the directly bonded imidazole nitrogens;^{24–26} in the (Cys)₃(His)₁-coordinated [2Fe-2S] cluster in the human mitochondrial protein (**18**), $e^2qQ/h = (-)2.47$ MHz;²⁷ and in several (Cys)₂(His)₂-coordinated [2Fe-2S] Rieske-type proteins (**19**), e^2qQ/h values have been reported to be in the range ~ 2.2 –2.9 MHz.^{28–30} Clearly then, the ^{14}N nuclear quadrupole coupling constant decreases from ~ 4 MHz for the free (gas phase) imidazole to ~ 2.5 MHz when imidazole is bound to Fe, similar to the decrease in e^2qQ/h we find with pyr bound to Fe in the 4Fe-4S cluster of IspH.

These results all support the idea that the IspH pyridine inhibitors bind to IspH via a Lewis acid/base (Fe_4S_4 cluster/ligand) mechanism, with the donor orbital occupancy (σ) decreasing from 2 (pyridine) to ~ 1.73 ,²⁰ and that the hyperfine coupling seen experimentally is due to this η^1 -bonding, rather than being due to a neutral pyr or pyr- H^+ ligand just being close to the 4Fe-4S cluster. This, in turn, suggests that stronger Lewis bases (such as imidazole-containing ligands) may be more potent IspH inhibitors. These results also support the idea that other inhibitors, such as alkynes,^{10,13} as well as possible reaction

intermediates (η^3 -alkyls),^{10,11} also act as Lewis bases when interacting with the 4Fe-4S cluster in IspH.

Overall, these results are of interest for several reasons. First, we find evidence for an ^{14}N HYSCORE signal when the pyridine inhibitor **7** binds to IspH. On the basis of isotopic labeling, this signal is assigned to the pyridine ^{14}N . Second, the experimental e^2qQ/h (from simulations of field-dependent HYSCORE) is 3 MHz. This is between the $e^2qQ/h = 4.6$ MHz found for pyridine itself and e^2qQ/h values of ~ 1 MHz found in pyridinium salts and pyridine-*N*-oxide²⁰ and, in fact, within the 2.4–3.1 MHz range of values found for pyridines bound to Cr, Mo, and Fe carbonyls.²³ So, while the ligand may initially bind as the cationic species (e.g., to E126), the η^1 -complex is the more stable species. Third, we report the results of DFT calculations of the ^{14}N nuclear quadrupole coupling constant (e^2qQ/h) in pyridine-containing metal systems, finding a good correlation between theory and experiment ($R^2 = 0.965$, slope = 0.963, Figure 2), in addition to predicting a 2.3 MHz e^2qQ/h value for a $[\text{Fe}_4\text{S}_4(\text{SMe})_3(\text{pyr})]^{2-}$ model cluster, in quite good accord with experiment (given that the protein was excluded from the calculation and the crystallographic structure of the 4Fe-4S/pyridine protein-containing complex is not yet known). When all published experimental results on pyridine- and imidazole-containing systems are considered, there is a ~ 35 –40% decrease in the ^{14}N e^2qQ/h on metal binding, the same as that found in the IspH + **7** system. This again supports formation of an η^1 -complex between IspH and **7**, an observation of interest in the context of the design of other inhibitors, of interest as anti-infective drug leads.

■ ASSOCIATED CONTENT

S Supporting Information. Details on protein production and purification, HYSCORE sample preparation, supporting figures, and complete ref 21. This material is available free of charge via the Internet at <http://pubs.acs.org>.

■ AUTHOR INFORMATION

Corresponding Author
eo@chad.scs.uiuc.edu

■ ACKNOWLEDGMENT

We thank Hassan Jomaa and Jochen Wiesner for providing their IspH plasmid. This work was supported by the United States Public Health Service (NIH grants AI074233 and GM065307). W.W. was supported by a Predoctoral Fellowship from the American Heart Association, Midwest Affiliate (Award 10PRE4430022). EPR instrumentation used in this work was supported by NIH grants S10RR023614 and S10RR025438, NSF CHE-0840501, and NCBC 2009-IDG-1015. Computational research was supported by the National Science Foundation through Teragrid resources provided by NCSA under grant TG-CHE100060.

■ REFERENCES

- Oldfield, E. *Acc. Chem. Res.* **2010**, *43*, 1216–1226.
- Rohmer, M. *Lipids* **2008**, *43*, 1095–1107.
- Rohmer, M.; Grosdemange-Billiard, C.; Seemann, M.; Tritsch, D. *Curr. Opin. Invest. Drugs* **2004**, *5*, 154–162.
- Hecht, S.; Eisenreich, W.; Adam, P.; Amslinger, S.; Kis, K.; Bacher, A.; Arigoni, D.; Rohdich, F. *Proc. Natl. Acad. Sci. U.S.A.* **2001**, *98*, 14837–14842.

- (5) Kollas, A. K.; Duin, E. C.; Eberl, M.; Altincicek, B.; Hintz, M.; Reichenberg, A.; Henschker, D.; Henne, A.; Steinbrecher, I.; Ostrovsky, D. N.; Hedderich, R.; Beck, E.; Jomaa, H.; Wiesner, J. *FEBS Lett.* **2002**, *532*, 432–436.
- (6) Seemann, M.; Bui, B. T. S.; Wolff, M.; Tritsch, D.; Campos, N.; Boronat, A.; Marquet, A.; Rohmer, M. *Angew. Chem. Int. Ed.* **2002**, *41*, 4337–4339.
- (7) Altincicek, B.; Duin, E. C.; Reichenberg, A.; Hedderich, R.; Kollas, A. K.; Hintz, M.; Wagner, S.; Wiesner, J.; Beck, E.; Jomaa, H. *FEBS Lett.* **2002**, *532*, 437–440.
- (8) Wolff, M.; Seemann, M.; Bui, B. T. S.; Frapart, Y.; Tritsch, D.; Garcia Estrabot, A.; Rodriguez-Concepcion, M.; Boronat, A.; Marquet, A.; Rohmer, M. *FEBS Lett.* **2003**, *541*, 115–120.
- (9) Wang, W.; Li, J.; Wang, K.; Huang, C.; Zhang, Y.; Oldfield, E. *Proc. Natl. Acad. Sci. U.S.A.* **2010**, *107*, 11189–11193.
- (10) Wang, W.; Wang, K.; Liu, Y.-L.; No, J. H.; Nilges, M. J.; Oldfield, E. *Proc. Natl. Acad. Sci. U.S.A.* **2010**, *107*, 4522–4527.
- (11) Grawert, T.; Span, I.; Eisenreich, W.; Rohdich, F.; Eppinger, J.; Bacher, A.; Groll, M. *Proc. Natl. Acad. Sci. U.S.A.* **2010**, *107*, 1077–1081.
- (12) Batsanov, S. *Inorg. Mater.* **2001**, *37*, 871–885.
- (13) Wang, K.; Wang, W.; No, J. H.; Zhang, Y.; Zhang, Y.; Oldfield, E. *J. Am. Chem. Soc.* **2010**, *132*, 6719–6727.
- (14) Rekkittke, I.; Wiesner, J.; Rohrich, R.; Demmer, U.; Warkentin, E.; Xu, W.; Troschke, K.; Hintz, M.; No, J. H.; Duin, E. C.; Oldfield, E.; Jomaa, H.; Ermler, U. *J. Am. Chem. Soc.* **2008**, *130*, 17206–17207.
- (15) Stoll, S.; Schweiger, A. *J. Magn. Reson.* **2006**, *178*, 42–55.
- (16) Fittipaldi, M.; Garcia-Rubio, I.; Trandafir, F.; Gromov, I.; Schweiger, A.; Bouwen, A.; Van Doorslaer, S. *J. Phys. Chem. B* **2008**, *112*, 3859–3870.
- (17) Vinck, E.; Van Doorslaer, S. *Phys. Chem. Chem. Phys.* **2004**, *6*, 5324–5330.
- (18) Dikanov, S. A.; Shubin, A. A.; Kounosu, A.; Iwasaki, T.; Samoilova, R. I. *J. Biol. Inorg. Chem.* **2004**, *9*, 753–767.
- (19) Lees, N. S.; Hanzelmann, P.; Hernandez, H. L.; Subramanian, S.; Schindelin, H.; Johnson, M. K.; Hoffman, B. M. *J. Am. Chem. Soc.* **2009**, *131*, 9184–9185.
- (20) Brown, T. L. *Inorg. Chem.* **1980**, *19*, 392–398.
- (21) Frisch, M. J.; *Gaussian 09*, Revision A.01; Gaussian, Inc.: Wallingford, CT, 2009.
- (22) Palmer, M. H.; Stephenson, D.; Smith, J. A. S. *Chem. Phys.* **1985**, *97*, 103–111.
- (23) Ashby, C. I. H.; Cheng, C. P.; Brown, T. L. *J. Am. Chem. Soc.* **1978**, *100*, 6057–6063.
- (24) Scholes, C. P.; Lapidot, A.; Mascarenhas, R.; Inubushi, T.; Isaacson, R. A.; Feher, G. *J. Am. Chem. Soc.* **1982**, *104*, 2724–2735.
- (25) Magliozzo, R. S.; Peisach, J. *Biochemistry* **1992**, *31*, 189–99.
- (26) Magliozzo, R. S.; Peisach, J. *Biochemistry* **1993**, *32*, 8446–56.
- (27) Dicus, M. M.; Conlan, A.; Nechushtai, R.; Jennings, P. A.; Paddock, M. L.; Britt, R. D.; Stoll, S. *J. Am. Chem. Soc.* **2010**, *132*, 2037–2049.
- (28) Britt, R. D.; Sauer, K.; Klein, M. P.; Knaff, D. B.; Kriauciunas, A.; Yu, C. A.; Yu, L.; Malkin, R. *Biochemistry* **1991**, *30*, 1892–1901.
- (29) Shergill, J. K.; Joannou, C. L.; Mason, J. R.; Cammack, R. *Biochemistry* **1995**, *34*, 16533–16542.
- (30) Gurbiel, R. J.; Batie, C. J.; Sivaraja, M.; True, A. E.; Fee, J. A.; Hoffman, B. M.; Ballou, D. P. *Biochemistry* **1989**, *28*, 4861–7481.